

# Wavelet Based Dictionaries for Dimensionality Reduction of ECG Signals

Laura Rebollo-Neira

Mathematics Department Aston University  
B3 7ET, Birmingham, UK

Dana Černá

Technical University of Liberec  
Liberec, Czech Republic

November 15, 2018

## Abstract

Dimensionality reduction of ECG signals is considered within the framework of sparse representation. The approach constructs the signal model by selecting elementary components from a redundant dictionary via a greedy strategy. The proposed wavelet dictionaries are built from the multiresolution scheme, but translating the prototypes within a shorter step than that corresponding to the wavelet basis. The reduced representation of the signal is shown to be suitable for compression at low level distortion. In that regard, compression results are superior to previously reported benchmarks on the MIT-BIH Arrhythmia data set.

## 1 Introduction

Electrocardiography (ECG) is the process of recording the electrical activity of the heart over a period of time. The overall goal of the test is to obtain information about the structure and function of that organ. Dimensionality reduction of ECG signals is relevant to techniques for analysis and classification of this type of data. Such techniques are subject of ongoing research [1–9], which includes methodologies based on the theory of compressive sensing [10–14].

Compressive sensing enhances the concept of sparsity by associating it to a new framework for digitalization [15,16]. Producing sparse representation of ECG signals is the central aim of the present work. This implies to represent an ECG record as superposition of as few elementary components as possible. The same goal was traditionally accomplished by disregarding the least significant terms in the wavelet transform of the signal [17]. However, as shown in this work, much less elementary components are necessary if they are selected from a redundant wavelet dictionary rather than from

a wavelet basis. This allows us to project an ECG record onto a subspace of lower dimensionality, in comparison to the dimension of the signal, and still reconstruct the record at low level distortion.

The main contributions of the paper are listed below:

- A number of wavelets dictionaries, based on existing families of wavelet bases, are developed.
- Each dictionary is shown to render much higher levels of sparsity for representing ECG signals than the corresponding basis. The tests are performed on the MIT-BIH Arrhythmia data set consisting of 48 records each of which of 30 min length.
- A strategy for storing the reduced representation of an ECG signal is considered. The resulting file is shown to render higher compression ratio than previously reported benchmarks on the same data set.
- MATLAB software for constructing the dictionaries, as well as for reproducing results, has been made available on a dedicated website [18].

The paper is organized as follows: Sec. 2 recalls the main ideas involved in the construction of wavelet dictionaries for Cardinal Spline Spaces. Sec. 3 introduces all the elements to build the model for dimensionality reduction of an ECG signal, and describes a strategy to store the reduced representation. Sec. 4 presents the numerical results. The conclusions are summarized in Sec. 5.

## 2 Wavelet Dictionaries

The proposed wavelet dictionaries are inspired on the construction of dictionaries for Cardinal Spline Spaces (CSS) as discussed in previous works [19–21]. Let us denote  $V_j, j \geq 0$  to the CSS of order  $m$  with simple knots at the equidistant partition of the interval  $[c, d]$  having distance  $2^{-j}$  between two adjacent knots. A basis for  $V_j$  arises from the restriction of the functions

$$\phi_{j,k}(x) := 2^{j/2} \phi(2^j x - k), k \in \mathbb{Z} \quad (1)$$

to the interval  $[c, d]$ , which we expressed as  $2^{j/2} \phi(2^j x - k)|_{[c,d]}$ . The function  $\phi(x) \equiv \phi_{0,0}(x)$  is called scaling function. For a CSS  $\phi(x)$  is the cardinal B-spline of order  $m$  associated with the uniform simple knot sequence  $0, 1, \dots, m$  [22]

$$\phi(x) = \frac{1}{m!} \sum_{i=0}^m (-1)^i \binom{m}{i} (x - i)_+^{m-1}, \quad (2)$$

where  $(x - i)_+^{m-1}$  is equal to  $(x - i)^{m-1}$  if  $x - i > 0$  and 0 otherwise.

The complementary wavelet subspace  $W_j$  on  $[c, d]$  is constructed in order to fulfil

$$V_{j+1} = V_j \oplus W_j, \quad j \in \mathbb{Z}^+, \quad (3)$$

so that

$$V_{j+1} = V_0 \oplus W_0 \oplus W_1 \oplus \cdots \oplus W_j. \quad (4)$$

For a given value of  $j$  a wavelet basis for  $W_j$  arises as

$$\psi_{j,k}(x) = 2^{j/2} \psi(2^j x - k)|_{[c,d]}, \quad k \in \mathbb{Z} \quad (5)$$

and the elimination of some redundancy introduced by the cutting process at the borders of the interval. Different constructions of mother wavelets  $\psi \equiv \psi_{0,0}$  give rise to different wavelet bases.

Within the multi-resolution framework, dictionaries for a CSS are simply constructed from the result asserting that if for  $l \in \mathbb{Z}^+$

$$\mathcal{W}_{j,l} = \{2^{j/2} \psi(2^j x - \frac{k}{2^l})|_{[c,d]}, \quad k \in \mathbb{Z}\}, \quad (6)$$

then [21]

$$\text{span}\{\mathcal{W}_{j,l}\} = V_{j+l}. \quad (7)$$

This result facilitates a tool for designing dictionaries of wavelets of different support spanning the same CSS. A multi-resolution-like dictionary  $\mathcal{D}_{j,l}$  spanning  $V_j$  is constructed as

$$\mathcal{D}_{j,\ell} = \mathcal{V}_{0,\ell} \cup \mathcal{W}_{0,\ell} \cup \mathcal{W}_{1,\ell} \cup \cdots \cup \mathcal{W}_{j-\ell,\ell}, \quad (8)$$

with

$$\mathcal{V}_{0,\ell} = \{\phi(x - \frac{k}{2^\ell})|_{[c,d]}, \quad k \in \mathbb{Z}\}. \quad (9)$$

The top graph of Fig. 1 shows consecutive wavelets in a cubic Chui-Wang4 [23] wavelet basis and consecutive wavelets in a dictionary for the same CSS. Notice that the wavelet functions at the finest scale in the dictionary are broader than those at the finest scale in the basis.

### 3 Piecewise model of an ECG signal

In the discrete case dictionaries can be constructed in a very simple manner: A redundant dictionary for the Euclidean space  $\mathbb{R}^N$  is simply any set of normalized vectors  $\{\mathbf{d}_i \in \mathbb{R}^N, \|\mathbf{d}_i\| = 1\}_{i=1}^M$  such that  $N$  of them are linearly independent and  $M > N$ . Inspired by the results for CSS we construct a dictionary for  $\mathbb{R}^N$  simply by discretization of the functions in the wavelet dictionary. Moreover, since

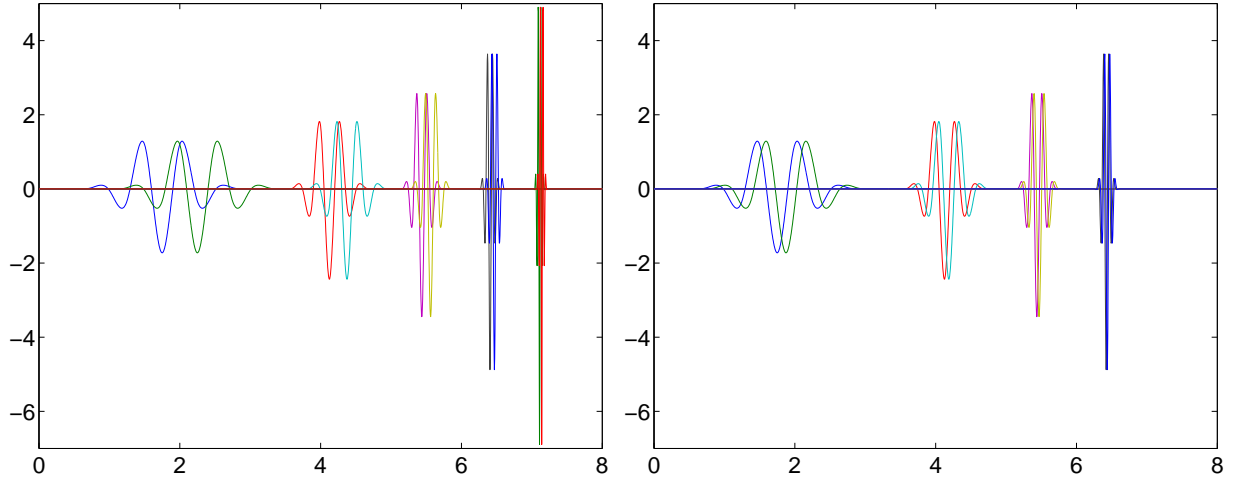


Figure 1: Wavelet functions taken from a basis for a CSS (left graph) and from a dictionary spanning the same CSS (right graph).

ECG signals are commonly superimposed to a smooth background we enrich a wavelet dictionary adding a few low frequency components from a discrete cosine basis.

Assuming that an ECG record is given as an array  $\mathbf{f}$  of dimension  $N$  we divide the signal into  $Q$  disjoint segments  $\mathbf{f}_q \in \mathbb{R}^{N_b}$ ,  $q = 1, \dots, Q$  and construct an approximation  $\mathbf{f}^{k_q}$  for each segment as the  $k_q$ -term ‘atomic decomposition’

$$\mathbf{f}^{k_q} = \sum_{n=1}^{k_q} c_q(n) \mathbf{d}_{\ell_n^q}, \quad (10)$$

where the elements  $\mathbf{d}_{\ell_n^q}$ , called ‘atoms’, are chosen from a given dictionary through a greedy pursuit strategy. Here for the selection process we adopt the Optimized Orthogonal Matching Pursuit (OOMP) method [24, 25] which is stepwise optimal in the sense of minimizing the residual norm  $\|\mathbf{f}_q - \mathbf{f}^{k_q}\|$  at each iteration. The algorithm evolves by selecting the atoms one by one until for fixed tolerance parameter,  $\rho$  say, the condition  $\|\mathbf{f} - \mathbf{f}^{k_q}\| < \rho$  is reached. For the reader convenience in Appendix A we have described the approximation algorithm, as it is implemented in the software supporting the paper. The complexity of the method, dominated by the selection of atoms, is  $O(KN_bM)$  with  $K = \sum_{q=1}^Q k_q$ .

Once all the segments  $\mathbf{f}_q$  have been approximated, the approximation of the whole signal is obtained by assembling the approximation of the segments as  $\mathbf{f}^r = \hat{\mathbf{J}}_{q=1}^Q \mathbf{f}^{k_q}$ , where  $\hat{\mathbf{J}}$  is the concatenation operation.

### 3.1 Encoding the signal model

For the reduced representation of the signal (10) to be suitable for storage and transmission purposes it is necessary to encode it within a small file in relation to the size of the original record. For this end, firstly the absolute value coefficients  $|c_q(n)|$ ,  $n = 1 \dots, k_q$ ,  $q = 1, \dots, Q$ , are converted into integers as follows:

$$c_q^\Delta(n) = \lfloor \frac{|c_q(n)|}{\Delta} + \frac{1}{2} \rfloor, \quad (11)$$

where  $\lfloor x \rfloor$  indicates the largest integer number smaller or equal to  $x$  and  $\Delta$  is the quantization parameter. The signs of the coefficients, represented as  $\mathbf{s}_q$ ,  $q = 1, \dots, Q$ , are encoded separately using a binary alphabet. For creating the strings of numbers to encode the the signal model we proceed as in [26, 27].

The indices of the atoms in the atomic decompositions of each block  $\mathbf{f}_q$  are first sorted in ascending order  $\ell_i^q \rightarrow \tilde{\ell}_i^q$ ,  $i = 1, \dots, k_q$ , which guarantees that, for each  $q$  value,  $\tilde{\ell}_i^q < \tilde{\ell}_{i+1}^q$ ,  $i = 1, \dots, k_q - 1$ . The order of the indices induces order in the unsigned coefficients,  $\mathbf{c}_q^\Delta \rightarrow \tilde{\mathbf{c}}_q^\Delta$  and in the corresponding signs  $\mathbf{s}_q \rightarrow \tilde{\mathbf{s}}_q$ . The ordered indices are stored as smaller positive numbers by taking differences between two consecutive values. By defining  $\delta_i^q = \tilde{\ell}_i^q - \tilde{\ell}_{i-1}^q$ ,  $i = 2, \dots, k_q$  the follow string stores the indices for block  $q$  with unique recovery  $\tilde{\ell}_1^q, \delta_2^q, \dots, \delta_{k_q}^q$ . The number ‘0’ is then used to separate the string corresponding to different blocks and entropy code a long string,  $st_{\text{ind}}$ , which is built as

$$st_{\text{ind}} = [\tilde{\ell}_1^1, \dots, \delta_{k_1}^1, 0, \tilde{\ell}_1^2, \dots, \delta_{k_2}^2, 0, \dots, \tilde{\ell}_1^{k_Q}, \dots, \delta_{k_Q}^{k_Q}]. \quad (12)$$

The corresponding quantized magnitude of the coefficients are concatenated in the strings  $st_{\text{cf}}$  as follows:

$$st_{\text{cf}} = [\tilde{c}_1^\Delta(1), \dots, \tilde{c}_1^\Delta(k_1), \dots, \tilde{c}_{k_Q}^\Delta(1), \dots, \tilde{c}_{k_Q}^\Delta(k_Q)]. \quad (13)$$

Using ‘0’ to store a positive sign and ‘1’ to store negative one, the signs are placed in the string,  $st_{\text{sg}}$  as

$$st_{\text{sg}} = [\tilde{s}_1(1), \dots, \tilde{s}_1(k_1), \dots, \tilde{s}_{k_Q}(1), \dots, \tilde{s}_{k_Q}(k_Q)]. \quad (14)$$

In the first instance, for the test in Sec. 4.2, we store these strings in hierarchical data format [28], simply using the MATLAB instruction `save`. For further improvement, when comparing compression performance in the test of Sec. 4.3, an entropy encoding step to store the strings at fixed bit depth is included.

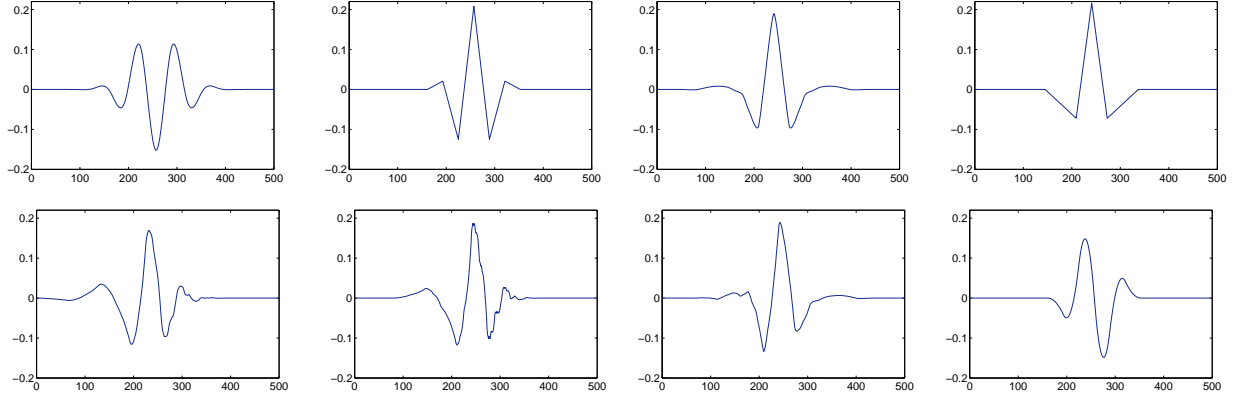


Figure 2: Wavelet prototypes. From left top to right bottom the graphs correspond to the families **CW4**, **CW2**, **CDF97**, **CDF53**, **Db4**, **Coif**, **Sym**, and **Short3**.

### 3.2 The Dictionary

As already mentioned, for approximating ECG signals the dictionaries we use are constructed as  $\mathcal{D} = \mathcal{D}^C \cup \mathcal{D}^W$ , where  $\mathcal{D}^W$  is a discrete wavelet basis (or dictionary) for  $\mathbb{R}^{N_b}$  and

$$\mathcal{D}^C = \{w_c(n) \cos \frac{\pi(2i-1)(n-1)}{2M}, i = 1, \dots, N_b\}_{n=1}^M.$$

Here we fix  $M = 10$ .

In the next section we perform the numerical tests by considering a number of different wavelet dictionaries, all obtained from previously derived wavelets bases.

For the sake of comparison we have built dictionaries for the following wavelet families.

**Semi-orthogonal spline wavelets** were already mentioned in a previous section. Their construction was proposed by C. Chui and J. Wang in [23]. Semi-orthogonal wavelets, also called prewavelets, are not orthogonal if the wavelets are at the same scale level, but orthogonality of wavelets at the different levels is preserved. Here we consider the cubic and linear cases, which are indicated as **CW4** and **CW2** respectively. The wavelet prototypes corresponding to this family are given the 1st and 2nd graphs in the 1st row Fig. 2.

**Cohen-Daubechies-Feauveau biorthogonal wavelets** were built in [29]. In this case both primal and dual wavelets have compact support. Wavelets from this family with 9 and 7 taps filters (**CDF97**) and with 5 and 3 taps filters (**CDF53**) are used in the JPEG2000 compression standard. The corresponding prototypes are given in the 3rd and 4th graphs of the 1st row of Fig. 2.

**Daubechies wavelets** were built by I. Daubechies as first orthonormal compactly supported continuous wavelets in [32]. They have the shortest possible support for the given number of vanishing moments and they have extremal phase. Here we consider the four vanishing moments and indicate it as **Db4**. This wavelet prototype is displayed in the 1st graph of the 2nd row of Fig. 2.

**Coiflets** were suggested by R. Coifman as orthonormal wavelet systems with vanishing moments for both scaling functions and wavelets. They were first constructed by I. Daubechies in [33]. We consider two vanishing moments used exact values of scaling and wavelet parameters from [34] and indicate the family as **Coif**. The mother wavelet is displayed in the 2nd graph in the 2nd row of Fig. 2.

**Symlets** are modified version of Daubechies wavelets. They have also the shortest possible support for the given number of vanishing moments, see [33]. We consider four vanishing moments. The prototype wavelet for the family **Sym** is given in the 3rd graph in the 2nd row of Fig. 2.

**Spline wavelets with short support** are obtained if the local support of dual wavelets is not required. They were designed in [30, 31]. Here we consider quadratic splines and indicate them as **Short3**. The prototype for this family is plotted in last graph of the 2nd row of Fig. 2.

## 4 Numerical tests

The numerical tests we present here use the full MIT-BIH Arrhythmia database [35] which contains 48 ECG records. Each of these records is of 30 min length, consisting of  $N = 650000$  11-bit samples at a frequency of 360 Hz.

All our results have been obtained in the MATLAB environment using a notebook 2.9GHz dual core i7 3520M CPU and 4GB of memory.

### 4.1 Assessment Metrics

The quality of the signal approximation is assessed with respect to the PRD calculated as follows,

$$\text{PRD} = \frac{\|\mathbf{f} - \mathbf{f}^r\|}{\|\mathbf{f}\|} \times 100\% \quad (15)$$

where,  $\mathbf{f}$  is the original signal and  $\mathbf{f}^r$  is the signal reconstructed from the approximated segments. Since the PRD strongly depends on the background of the signal, the PRDN, as defined below, is also a relevant metric.

$$\text{PRDN} = \frac{\|\mathbf{f} - \mathbf{f}^r\|}{\|\mathbf{f} - \bar{\mathbf{f}}\|} \times 100\%, \quad (16)$$

where,  $\bar{\mathbf{f}}$  indicates the mean value of  $\mathbf{f}$ .

For a fixed value of PRD the sparsity of a representation is measure by the sparsity ratio (SR)

$$\text{SR} = \frac{N}{K}, \quad (17)$$

where  $N$  is the total length of the signal and  $K = \sum_{q=1}^Q k_q$ , with  $k_q$  the number of atoms in the atomic decomposition (10) of each segment. The compression performance depends of the size of the

file storing the signal representation and is assessed by the Compression Ratio (CR) as given by

$$\text{CR} = \frac{\text{Size of the uncompressed file.}}{\text{Size of the compressed file}} \quad (18)$$

The quality score (QS), reflecting the tradeoff between compression performance and reconstruction quality, is the ratio:

$$\text{QS} = \frac{\text{CR}}{\text{PRD}}. \quad (19)$$

Since the PRD is a global quantity, in order to detect possible local changes in the visual quality of the recovered signal, we consider the local PRD as follows. Each signal is partitioned in  $Q$  segments  $\mathbf{f}_q$ ,  $q = 1 \dots, Q$  of  $L$  samples. The local PRD with respect to every segment in the partition is indicate as  $\text{prd}(q)$ ,  $q = 1, \dots, Q$ , calculated as

$$\text{prd}(q) = \frac{\|\mathbf{f}_q - \mathbf{f}_q^r\|}{\|\mathbf{f}_q\|} \times 100\%, \quad (20)$$

where  $\mathbf{f}_q^r$  is the recovered portion of the signal corresponding to the segment  $q$ . In all the numerical test of the next section the OOMP approximation is carried out up to a fixed value  $\rho$  so as to achieve the same value of  $\text{prd}$  for all the segments in the records. Assuming that the target  $\text{prd}$  before quantization is  $\text{prd}_0$  we set  $\rho = \text{prd}_0 \|\mathbf{f}_q\| / 100$ .

## 4.2 Test I

The purpose of the first numerical tests is to demonstrate the significant gain in dimensionality reduction (high values of SR) achieved if the component  $\mathcal{D}^W$  of the dictionary  $\mathcal{D}$  is a wavelet dictionary instead of a wavelet basis. The wavelet basis arises using as translation parameter  $b = 1$  and the wavelet dictionary using a translation parameter  $b = 1/4$ . A wavelet basis contains scales corresponding to the values  $j = 3, \dots, 8$  while the corresponding dictionary contains one less scale i.e.  $j = 3, \dots, 7$ . The exact redundancy of the dictionary depends of the wavelet family but in all the cases is close to two. The records are approximated by partitioning the signal into  $Q = 1300$  segments of  $N_b = 500$  data points each.

The second column in Table 1 gives the mean value SR, after quantization, with respect to the 48 records in the data set. The standard deviation is given in the 3rd column. The approximation with all the families is carrier out to obtain the same mean value of PRD ( $\overline{\text{PRD}} = 53$ ). For this test the quantization parameter is fixed. For all the records and all the dictionaries  $\Delta = 35$ . The 4th column gives the mean value CR and the fifth column the corresponding standard deviation. The 1st column lists the different wavelet families which are considered to build the dictionary  $\mathcal{D}^W$ . The subscript B is used to indicate the wavelet basis and the subscript D to indicate the corresponding



Table 1: Mean values of SR and CR with respect to the 48 records in the MIT-BIH Arrhythmia database. In all the cases the reconstructed signals produce  $\overline{\text{PRD}} = 53$ .

$\mathcal{D}^w$	$\overline{\text{SR}}$	std	$\overline{\text{CR}}$	std
<b>CW4<sub>B</sub></b>	10.13	2.42	11.72	3.16
<b>CW4<sub>D</sub></b>	16.62	4.13	13.31	3.51
<b>CW2<sub>B</sub></b>	11.34	2.91	12.14	3.48
<b>CW2<sub>D</sub></b>	16.76	4.95	13.92	4.04
<b>CDF97<sub>B</sub></b>	14.59	3.90	14.88	4.20
<b>CDF97<sub>D</sub></b>	<b>20.60</b>	5.79	<b>16.20</b>	4.51
<b>CDF53<sub>B</sub></b>	14.72	4.25	14.99	4.29
<b>CDF53<sub>D</sub></b>	<b>20.18</b>	6.36	<b>16.02</b>	4.88
<b>Db4<sub>B</sub></b>	12.81	3.28	13.51	3.62
<b>Db4<sub>D</sub></b>	17.88	4.94	14.24	4.05
<b>Coif<sub>B</sub></b>	11.50	2.99	12.62	3.47
<b>Coif<sub>D</sub></b>	15.27	4.57	12.58	3.68
<b>Sym<sub>B</sub></b>	12.83	3.30	13.62	3.66
<b>Sym<sub>D</sub></b>	18.41	5.22	14.63	4.22
<b>Short3<sub>B</sub></b>	12.78	3.18	15.35	4.31
<b>Short3<sub>D</sub></b>	<b>19.84</b>	5.25	<b>16.01</b>	4.24

dictionary, i.e. **CDF97<sub>B</sub>** indicates the 9/7 Cohen-Daubechies-Feauveau biorthogonal wavelet basis and **CDF97<sub>D</sub>** the corresponding wavelet dictionary.

As seen in Table 1 the best results in relation to dimensionality reduction (largest values of  $\overline{\text{SR}}$ ) and compression (largest values of  $\overline{\text{CR}}$ ) are for **CDF97<sub>D</sub>**, **CDF53<sub>D</sub>** and **Short3<sub>D</sub>**. In terms of dimensionality reduction all the wavelet bases perform poorly in comparison to the dictionaries. The difference in  $\overline{\text{CR}}$  is not so pronounced though. This is because, in spite of the fact that the approximation using a dictionary involves much less elementary components in the signal decomposition, the dispersion of indices corresponding to the atoms in the decomposition is larger if using a dictionary.

Since the storage strategy we have adopted benefits from the concentration in the location of indices, the gain in  $\overline{\text{CR}}$  is not as significant as the gain in  $\overline{\text{SR}}$ . The latter quantity is relevant to methodologies relying on dimensionality reduction of ECG signals for classification and recognition tasks [36,37]. For further information in Table 2 we provide the figures of the evaluation metrics for each of the 48 records in the dataset.

The 2nd column of Table 2 shows the values of PRD for the records listed in the 1st column. The 3rd column shows the values of SR after quantization. The CR is given in the 4th column and the

Table 2: Sparsity Ratio SR Compression Ratio CR and Quality Score QS for each of the 48 records in the MIT-BIH Arrhythmia Database listed in the first column.

Rec	PRD	SR	CR	QS	PRDN	Rec	PRD	SR	CR	QS	PRDN
100	0.51	27.19	21.43	42.16	12.64	202	0.51	26.24	20.33	40.03	8.44
101	0.51	25.39	19.73	38.71	9.45	203	0.55	12.75	9.74	19.09	5.54
102	0.51	24.43	18.87	36.72	13.13	205	0.51	25.25	20.64	40.33	12.50
103	0.52	21.93	16.93	32.72	7.86	207	0.51	25.93	20.06	39.63	7.08
104	0.53	19.00	14.04	28.56	10.27	208	0.54	15.09	12.00	22.24	5.55
105	0.53	17.37	13.92	26.21	6.43	209	0.54	15.65	12.68	23.60	9.92
106	0.53	18.63	14.43	27.43	7.07	210	0.51	23.84	18.82	36.76	9.72
107	0.55	12.64	9.84	17.82	3.18	212	0.56	12.12	10.212	18.33	8.35
108	0.52	21.13	17.12	32.70	8.51	213	0.56	11.71	9.31	16.72	4.09
109	0.52	19.32	15.21	29.00	5.16	214	0.52	19.22	14.76	28.18	5.54
111	0.51	23.22	18.45	35.89	9.90	215	0.55	14.07	11.57	21.23	9.60
112	0.53	22.72	18.91	35.57	10.20	217	0.53	16.86	12.78	24.04	4.30
113	0.52	20.21	15.29	29.34	6.26	219	0.54	18.06	13.90	25.92	4.43
114	0.50	32.21	25.33	50.55	14.52	220	0.53	19.18	15.00	28.15	7.65
115	0.53	20.18	15.71	29.73	6.73	221	0.52	22.73	17.55	34.02	8.50
116	0.58	12.33	9.10	15.59	3.72	222	0.51	26.52	20.91	41.25	13.53
117	0.52	27.31	21.88	41.78	9.33	223	0.53	18.56	14.48	27.10	6.06
118	0.59	11.06	8.77	14.84	5.90	228	0.52	18.97	15.37	29.38	7.53
119	0.56	16.15	12.66	22.78	4.44	230	0.52	19.12	14.96	28.59	7.30
121	0.51	33.27	26.12	51.22	7.29	231	0.51	25.67	20.04	39.60	9.23
122	0.56	16.42	13.32	23.99	6.50	232	0.50	29.72	23.81	48.02	14.91
123	0.53	21.94	17.33	32.56	7.94	233	0.54	14.26	11.36	20.98	4.96
124	0.53	23.28	17.88	33.94	4.94	234	0.52	19.81	15.76	30.15	7.68
200	0.53	15.56	12.60	23.60	7.05	<b>mean</b>	<b>0.53</b>	<b>20.60</b>	<b>16.20</b>	<b>31.08</b>	<b>7.99</b>
201	0.49	34.72	26.88	54.88	12.52	<b>std</b>	<b>0.02</b>	<b>5.79</b>	<b>4.54</b>	<b>9.69</b>	<b>2.92</b>

corresponding QS in the 5th column. The last column corresponds to the values of PRDN. All the results are obtained using the dictionary **CDF97<sub>D</sub>**. The average time for producing Table 2 is 27 s per record.

Fig. 3 depicts the approximation and raw data (indistinguishable in the scale of the graphs) of 2000 points in the records 107 and 116.

### 4.3 Test II

In this test we compare compression results with previously reported benchmarks on the MIT-BIH Arrhythmia database. Table 3 compares CRs obtain with **CDF97<sub>B</sub>**, **CDF97<sub>D</sub>**, **CDF53<sub>B</sub>**, **CDF53<sub>D</sub>**, **Short3<sub>B</sub>** and **Short3<sub>D</sub>** against those reported in [38] and [39] for the same mean values of PRD.

As anticipated, for further improvement in CR we add now an entropy coding step to save the

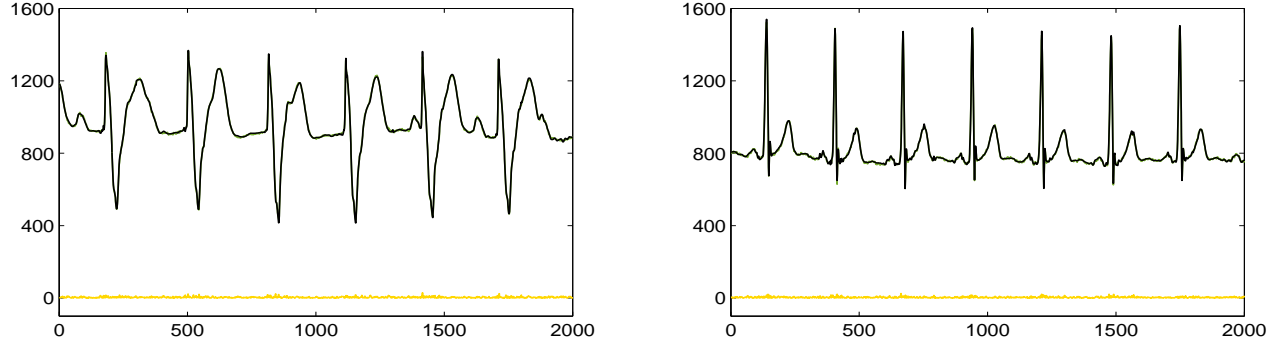


Figure 3: The waveforms in the graphs are the raw data and the approximations corresponding to 2000 points in the records 107 (left) and 116 (right). The bottom lines represent the absolute value of the difference between the data and the approximation.

Table 3: Comparison between the average compression performance of the proposed method and the methods in [38] and [39] for the same mean value of  $\overline{\text{PRD}}$ .

$\overline{\text{PRD}}$	0.91	0.80	0.67	0.48	0.31
$\overline{\text{CR}}$ [38]			11.30	9.28	6.22
$\overline{\text{CR}}$ [39]	22.27	18.00			
<b>CDF97<sub>B</sub></b>	24.21	21.82	18.41	13.64	8.48
<b>CDF97<sub>B</sub><sup>Hf</sup></b>	31.85	28.70	24.58	18.83	12.36
<b>CDF97<sub>D</sub></b>	26.27	23.81	20.52	14.79	9.37
<b>CDF97<sub>D</sub><sup>Hf</sup></b>	34.42	31.07	26.71	19.59	12.50
<b>CDF53<sub>B</sub></b>	25.25	22.87	19.21	13.61	8.33
<b>CDF53<sub>B</sub><sup>Hf</sup></b>	32.74	29.46	25.16	18.85	11.89
<b>CDF53<sub>D</sub></b>	27.30	24.50	20.67	14.67	8.89
<b>CDF53<sub>D</sub><sup>Hf</sup></b>	35.70	31.93	26.91	19.25	11.93
<b>Short3<sub>B</sub></b>	24.59	22.55	19.08	14.29	8.84
<b>Short3<sub>B</sub><sup>Hf</sup></b>	29.98	27.5	23.61	18.49	12.38
<b>Short3<sub>D</sub></b>	25.14	22.86	19.87	14.86	9.34
<b>Short3<sub>D</sub><sup>Hf</sup></b>	33.03	29.90	25.85	19.54	12.73
$\Delta$	80	60	40	30	16

strings described in Sec. 3.1 at a fixed bit depth using Huffman coding. The implementation of the step is realized using the off-the-shelf MATLAB function Huff06 available on [40]. The corresponding outcomes are indicated in Table 3 as **CDF97<sub>B</sub><sup>Hf</sup>**, **CDF97<sub>D</sub><sup>Hf</sup>**, **CDF53<sub>B</sub><sup>Hf</sup>**, **CDF53<sub>D</sub><sup>Hf</sup>**, **Short3<sub>B</sub><sup>Hf</sup>**, and **Short3<sub>D</sub><sup>Hf</sup>**. The last row gives the values of the quantization parameter  $\Delta$ . As seen in the table, the

entropy coding step improves the CR up to 45%. For  $\overline{\text{PRD}} = 0.48$  the average time for implementing this step is 5 s per record, while the average time for the OOMP approximation is 30 s per record. It follows from Tables 3 that, while the CR produced if  $\mathcal{D}^{\text{W}}$  is a basis is not very different from that produced if  $\mathcal{D}^{\text{W}}$  is a dictionary, the improvement with respect to previously reported results is substantial: On average an improvement of 115%, with respect to the results in [38], and an improvement of 66% with respect to the results in [39].

**Remark 1:** Because assessing the quality of an approximation by the PRD implies to focus on compression at low level distortion, we have restricted the values of PRD to the range [0.31 0.91]. However, in order to compare with [41], where results over-performing those in [39] for  $\overline{\text{PRD}} = 1.43$  have been recently reported, we have also compressed the database to produce  $\overline{\text{PRD}} = 1.43$ . Our results using  $\mathbf{CDF97}_{\text{D}}^{\text{Hf}}$  are  $\overline{\text{CR}} = 57.20$  with  $\overline{\text{QS}} = 40.71$ , while the results in [41] are  $\overline{\text{CR}} = 35.53$  with  $\overline{\text{QS}} = 33.41$ .

## 5 Conclusions

A method for dimensionality reduction of ECG signals has been proposed. The approach was designed within the framework of sparse representation. A number of wavelet based dictionaries have been introduced to undertake the signal model via the OOMP greedy strategy. The resulting representation was shown to require significantly less elementary component than those needed when using a wavelet basis. The method was proven to be useful for ECG compression at low level distortion. The compression results largely surpass recently reported benchmarks on the MIT-BIH Arrhythmia database.

The MATLAB software for constructing the dictionaries and reproducing the results in the paper has been made available on a dedicated website. Although the numerical construction of the signal model is computationally intensive it can be effectively realized, even in the MATLAB environment, where it typically takes 30 s to compress a 30 min record and 1 s to recover the signal from the compressed file. Moreover, since the approximation is carried out independently in every segment of the signal partition, there is room for straightforward parallelization using multiprocessors.

## Appendix A. OOMP method

Since ECG records are normally superimpose to a smooth background, we have initialized the OOMP algorithm by assuming that the constant atom is always one of the elements in (10). Hence, for each  $q$  we set  $k_q = 0$ ,  $\Gamma_q = \emptyset$ ,  $\ell_1^q = 1$ , and  $\mathbf{w}_1^q = \mathbf{b}_1^{1,q} = \mathbf{d}_1$ . Accordingly  $\mathbf{f}_1^q = \mathbf{d}_1 \langle \mathbf{f}_q, \mathbf{d}_1 \rangle$  (where  $\langle \cdot, \cdot \rangle$

indicates the Euclidean inner product), and  $\mathbf{r}_q^1 = \mathbf{f}_q - \mathbf{f}_q^1$ .

From the above initialization the OOMP approach for selecting the elements  $\mathbf{d}_{\ell_n^q}$ ,  $n = 2, \dots, k_q$  in (10) and calculating the corresponding coefficients  $c_q(n)$ ,  $n = 1, \dots, k_q$ , iterates as follows.

- 1) Upgrade the set  $\Gamma_q \leftarrow \Gamma_q \cup \ell_{k_q+1}$ , increase  $k_q \leftarrow k_q + 1$ , and select the index of a new atom for the approximation as

$$\ell_{k_q+1}^q = \arg \max_{\substack{n=1, \dots, M \\ n \notin \Gamma_q}} \frac{|\langle \mathbf{d}_n, \mathbf{r}_q^{k_q} \rangle|^2}{1 - \sum_{i=1}^{k_q} |\langle \mathbf{d}_n, \tilde{\mathbf{w}}_i^q \rangle|^2}, \quad (\text{A.1})$$

with  $\tilde{\mathbf{w}}_i^q = \frac{\mathbf{w}_i^q}{\|\mathbf{w}_i^q\|}$ .

- 2) Compute the corresponding new vector  $\mathbf{w}_{k_q+1}^q$  as

$$\mathbf{w}_{k_q+1}^q = \mathbf{d}_{\ell_{k_q+1}^q}^q - \sum_{n=1}^{k_q} \frac{\mathbf{w}_n^q}{\|\mathbf{w}_n^q\|^2} \langle \mathbf{w}_n^q, \mathbf{d}_{\ell_{k_q+1}^q}^q \rangle. \quad (\text{A.2})$$

including, for numerical accuracy, the re-orthogonalizing step:

$$\mathbf{w}_{k_q+1}^q \leftarrow \mathbf{w}_{k_q+1}^q - \sum_{n=1}^{k_q} \frac{\mathbf{w}_n^q}{\|\mathbf{w}_n^q\|^2} \langle \mathbf{w}_n^q, \mathbf{w}_{k_q+1}^q \rangle. \quad (\text{A.3})$$

- 3) For  $n = 1, \dots, k_q$  upgrade vectors  $\mathbf{b}_n^{k_q, q}$  as

$$\begin{aligned} \mathbf{b}_n^{k_q+1, q} &= \mathbf{b}_n^{k_q, q} - \mathbf{b}_{k_q+1}^{k_q+1, q} \langle \mathbf{d}_{\ell_{k_q+1}^q}^q, \mathbf{b}_n^{k_q+1, q} \rangle, \\ \mathbf{b}_{k_q+1}^{k_q+1, q} &= \frac{\mathbf{w}_{k_q+1}^q}{\|\mathbf{w}_{k_q+1}^q\|^2}. \end{aligned} \quad (\text{A.4})$$

- 4) Calculate

$$\mathbf{r}_q^{k_q+1} = \mathbf{r}_q^{k_q} - \langle \mathbf{w}_{k_q+1}^q, \mathbf{f}_q \rangle \frac{\mathbf{w}_{k_q+1}^q}{\|\mathbf{w}_{k_q+1}^q\|^2}. \quad (\text{A.5})$$

- 5) If for a given  $\rho$  the condition  $\|\mathbf{r}_q^{k_q+1}\| < \rho$  has been met compute the coefficients  $c_q(n) = \langle \mathbf{b}_n^{k_q}, \mathbf{f}_q \rangle$ ,  $n = 1, \dots, k_q$ . Otherwise repeat steps 1) - 5).

*Note:* Since for the adopted initialization the constant atom  $\mathbf{d}_1$  is forced to be in the signal decomposition, there is no need for storing the index  $\ell_1 = 1$ . Moreover, since the magnitude of the concomitant coefficients  $c_q(1)$ ,  $q = 1, \dots, k_q$  are normally much larger than the magnitude of the other coefficients, these are quantized with a parameter  $2\Delta$  and stored in a single string. After a shift of indices the remaining coefficients are stored as indicated in Sec. 3.1.

# Acknowledgments

We are indebted to Karl Skretting for making available the MATLAB functions `Huff06` which has been used for adding entropy coding to the proposed compression scheme.

# References

- [1] S. Banerjee, M. Mitra, “Application of Cross Wavelet Transform for ECG pattern analysis and classification”, *IEEE Transactions on Instrumentation and Measurement*, **63** 326–333 (2014).
- [2] R.G. Afkhami, G. Azarnia, M.A. Tinati, “Cardiac arrhythmia classification using statistical and mixture modeling features of ECG signals, *Pattern Recognition Letters*, **70**, 45– 51 (2016).
- [3] S. Shadmand, B. Mashoufi, “A new personalized ECG signal classification algorithm using block-based neural network and particle swarm optimization, *Biomedical Signal Processing and Control*, **25**, 12–23 (2016).
- [4] E.J.D. Luz, W.R. Schwartz, G. Camara-Chavez, D. Menotti, ECG-based heartbeat classification for arrhythmia detection: a survey, *Computer Methods and Programs in Biomedicine*, **127** 144–164 (2016).
- [5] D. P. Tobón V., T. H. Falk, M. Maier, “MS-QI: A Modulation Spectrum-Based ECG Quality Index for Telehealth Applications”, *IEEE Transactions on Biomedical Engineering*, **63**, 1613–1622 (2016).
- [6] S. Gutta, Q. Cheng, “Joint feature extraction and classifier design for ECG-based biometric recognition”, *Journal of Biomedical and Health Informatics*, **20**, 460–468 (2016).
- [7] H. Li, D. Yuan, Y. Wang, D. Cui, and L. Cao, “Arrhythmia Classification Based on Multi-Domain Feature Extraction for an ECG Recognition System”, *Sensors*, **16**, doi:10.3390/s16101744 (2015).
- [8] M. Abdelazez, P. X. Quesnel, A. D. C. Chan, H. Yang, “Signal Quality Analysis of Ambulatory Electrocardiograms to Gate False Myocardial Ischemia Alarms”, *IEEE Transactions on Biomedical Engineering*, **64**, 1318 – 1325 (2018).
- [9] S. K. Berkaya, A. K. Uysal, E. S. Gunal, S. Ergin., S. Gunal, M. B. Gulmezoglu, “A survey on ECG analysis”, *Biomedical Signal Processing and Control*, **43**, 216 – 235 (2018).

- [10] H. Mamaghanian, N. Khaled, D. Atienza and P. Vanderghenst, “Compressed Sensing for Real-Time Energy-Efficient ECG Compression on Wireless Body Sensor Nodes”, *IEEE Transactions on Biomedical Engineering*, **58**, 2456 – 2466 (2011).
- [11] Z. Zhang, T-P Jung, S. Makeig and B. D. Rao, “Compressed Sensing for Energy-Efficient Wireless Telemonitoring of Noninvasive Fetal ECG via Block Sparse Bayesian Learning”, *IEEE Transactions on Biomedical Engineering*, **60**, 300–309 (2013).
- [12] L. F. Polanía, R. E. Carrillo, Manuel Blanco-Velasco and K. E. Barner, “Exploiting Prior Knowledge in Compressed Sensing Wireless ECG Systems”, *IEEE Journal of Biomedical and Health Informatics*, **19**, 508–519 (2015).
- [13] G. Da Poian, R. Bernardini, R. Rinaldo, ‘RSeparation and Analysis of Fetal-ECG Signals From Compressed Sensed Abdominal ECG Recordings”, *IEEE Transactions on Biomedical Engineering*, **63**, 1269 – 1279 (2016).
- [14] L. F. Polanía and R. I. Plaza, “Compressed Sensing ECG using Restricted Boltzmann Machines”, *Biomedical Signal Processing and Control*, **45**, 237–45 (2018).
- [15] R. Baraniuk, “Compressive sensing”, *IEEE Signal Processing Magazine*, **24**, 118–121, (2007).
- [16] E. Candès and M. Wakin, “An introduction to compressive sampling”, *IEEE Signal Processing Magazine*, **25**, 21 – 30 (2008).
- [17] M. S Manikandan and S. Dandapat, “Wavelet-based electrocardiogram signal compression methods and their performances: A prospective review”, *Biomedical Signal Processing and Control*, **14**, 73–107 (2014).
- [18] <http://www.nonlinear-approx.info/examples/node011.html> (Last access Nov 2018).
- [19] M. Andrieu and L. Rebollo-Neira, “Cardinal B-spline dictionaries on a compact interval”, *Appl. Comput. Harmon. Anal.*, **18**, 336–346 (2005)
- [20] L. Rebollo-Neira and Z. Xu, “Adaptive non-uniform B-spline dictionaries on a compact interval”, *Signal Processing*, **90**, 2308–2313 (2010).
- [21] M. Andrieu and L. Rebollo-Neira, “From cardinal spline wavelet bases to highly coherent dictionaries”, *Journal of Physics A* **41** (2008) 172001.
- [22] L. L. Schumaker, *Spline Functions: Basic Theory*, Wiley, New-York, 1981.

- [23] C. Chui and J. Wang, “On compactly supported spline wavelets and a duality principle”, *Trans. Amer. Math. Soc.*, **330**, 903–915 (1992)
- [24] L. Rebollo-Neira and D. Lowe, “Optimized orthogonal matching pursuit approach”, *IEEE Signal Process. Letters*, **9**, 137–140 (2002).
- [25] L. Rebollo-Neira, “Cooperative greedy pursuit strategies for sparse signal representation by partitioning”, *Signal Processing*, **125**, 365–375 (2016).
- [26] L. Rebollo-Neira and I. Sanches, , “Simple scheme for compressing sparse representation of melodic music”, *Electronics Letters* (2017) DOI:10.1049/el.2017.3908
- [27] L. Rebollo-Neira, “A competitive scheme for storing sparse representation of X-Ray medical images” (2018) *PLOS ONE*. <https://doi.org/10.1371/journal.pone.0201455>.
- [28] L. A. Wasser, “Hierarchical Data Formats - What is HDF5?”, <https://www.neonscience.org/about-hdf5> (2015)
- [29] A. Cohen, I. Daubechies, and J.C. Feauveau, “Biorthogonal bases of compactly supported wavelets”, *Comm. Pure and Appl. Math.*, **45**, 485–560 (1992).
- [30] D. Chen, “Spline wavelets of small support”, *SIAM J. Math. Anal.*, **26**, 500–517 (1995).
- [31] B. Han and Z. Shen, “Wavelets with short support”, *SIAM J. Math. Anal.*, **38**, 530–556 (2006).
- [32] I. Daubechies, “Orthonormal bases of compactly supported wavelets”, *Commun. Pure Appl. Math.*, **41**, 909–996 (1988).
- [33] I. Daubechies, “Orthonormal bases of compactly supported wavelets II, variations on a theme”, *SIAM J. Math. Anal.*, **24**, 499–519 (1993).
- [34] D. Černá, V. Finěk, and K. Najzar, “On the exact values of coefficients of coiflets”, *Cent. European J. Math.* **6**, 159–169 (2008).
- [35] <https://physionet.org/physiobank/database/mitdb/> (Last access Nov 2018).
- [36] J. Wang, M. She, S. Nahavandi, A. Kouzani, “Human Identification From ECG Signals Via Sparse Representation of Local Segments”, *IEEE Signal Processing Letters*, **20**, 937 – 940 (2013).
- [37] S. Raj, K. C. Ray, “Sparse representation of ECG signals for automated recognition of cardiac arrhythmias”, *Expert Systems with Applications*, **105**, 49–64 (2018).



- [38] S.J. Lee, J. Kim and M. Lee, “A Real-Time ECG Data Compression and Transmission Algorithm for an e-Health Device”, *IEEE Transactions on Biomedical Engineering*, **58**, 2448–2455 (2011).
- [39] J.L. Ma, T.T. Zhang and M. C. Dong, “A Novel ECG Data Compression Method Using Adaptive Fourier Decomposition With Security Guarantee in e-Health Applications”, *IEEE Journal of Biomedical and Health Informatics*, **19**, 986–994 (2015).
- [40] K. Skretting, <http://www.ux.uis.no/~karlsk/proj99> (Last access Nov 2018).
- [41] C. Tan, L. Zhang and H. Wu, “A Novel Blaschke Unwinding Adaptive Fourier Decomposition based Signal Compression Algorithm with Application on ECG Signals”, *IEEE Journal of Biomedical and Health Informatics* 10.1109/JBHI.2018.2817192, 22 March 2018.